Supplementary Material

A Fully Verified Theoretical Analysis of Strain-Photonic Coupling for Quantum Well Embedded in Wavy Nanoribbons

Jiushuang Zhang[a,b], Yun Xu[a,b,], Yu Jiang[a,b], Lin Bai[a,b], Huamin Chen[a,b], Jian Li[a,b], Lei Wang[a,b], Weitong Wu[a,b], and Guofeng Song[a,b]*

[a] Institute of Semiconductors, Chinese Academy of Sciences, Beijing 100083, China

[b] College of Materials Science and Opto-Electronic Technology, University of Chinese Academy of Sciences, Beijing 101408, People's Republic of China.

S1. Experimental details

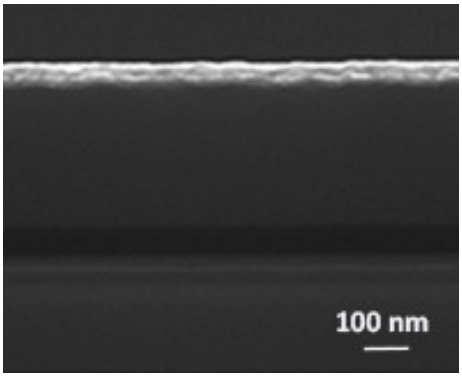

Figure S1-1. Scanning electron microscopy image of cross-section of the wavy QWNR. The bright and dark areas are Au and AlAs sacrificial layers respectively, with QW in the middle.

Preparation of the Quantum Well Nanoribbons in a Wavy Configuration. The fabrication of wavy quantum well nanoribbons starts with the deposition of functional materials by molecular beam epitaxy (MBE) on a native GaAs (001) substrate sequentially as AlAs/ $Al_{0.3}Ga_{0.7}As$/ GaAs/ $Al_{0.3}Ga_{0.7}As$ (100 nm/ 250 nm/ 6.5 nm/ 250 nm). The patterning process begins with the negative photoresist lithography, after which the patterned area with ribbons (90 μm wide and 2.5 mm long) on the epitaxy plate is empty. An additional layer of Au with thickness of 80 nm is then deposited on top using Vaccum Sputter Coater (DP 650, France). Clean the photoresist to strip the undesired gold off, hence only the designed gold ribbons are remained on top, meanwhile serving as a mask for the following wet etching process with mixed acid (85% H_3PO_4/ 30% H_2O_2/ deionized water = 2:1:10) for 30 s to form the quantum well nanoribbons on the substrate. Partially removing the AlAs sacrificial layer by HF acid (40% HF/ 100% ethanol = 1:2) for 1 min 30 s to suspend the nanoribbons on the mother wafer and ready for transfer printing. The soft substrate PDMS (Sylgard 184,

Dow Corning) mixed at weight ratio 10:1 is prepared in ultraviolet light for 3 min to clean and activate its surface in order to facilitate the printing process. Then pre-stretch the PDMS substrate by a bidirectional stretcher and stick the suspended ribbons onto the surface. Finally, peel the rigid substrate off and release the PDMS elastomer to finish the fabrication process. The cross-sectional image of wavy QNNR and 3D morphographic image of the sample are characterized by scanning microscope (SEM, FEI Quanta 450) and 3d laser microscope (VK-X 200 series).

μ-PL Measurements of the Wavy Quantum Well Nanoribbon. The steady-state PL spectra under the excitation of a 633 nm cw laser is collected by a microscope PL setup with Horiba Jobin Yvon iHR550 spectrometer. A HeNe laser (λ = 633 nm) is chosen to focus onto a single spot with a diameter of about 2 μm. Laser power is set to 0.06 mW in order to eliminate the possible cross-talk signal caused by the thermal effect. The micrometer-scale measurements ensure the precise reflection of the "in situ" information. Si CCD detector is chosen to detect the photoluminescence signals. Alternatively, the integrated PL of nanoribbon ensembles was collected using a 5× objective (Leica N-Plan, 15 μm spot diameter, large spot).

S2. Theoretical methods

From Eq. (4) and (5) in the main text, the whole Hamiltonian can be recast into a linear combination of terms that include all orders of k, which is written as,

$$\mathrm{H(k)} = \mathrm{H_{Bulk}(k)} + \mathrm{H_{Strain}} = \mathrm{H}_i^{(2)} k_i^2 + \mathrm{H}_i^{(1)} k_i + \mathrm{H}_i^{(0)} \tag{S2-1}$$

$$= \begin{pmatrix} A_{11} & A_{11} & \mathsf{L} & A_{11} \\ & A_{11} & & \mathsf{M} \\ & & \mathsf{O} & \mathsf{M} \\ H.c. & & & A_{11} \end{pmatrix}$$

where

$$A_{mn} = A^{(2)}_{mn,i} k_i^2 + A^{(1)}_{mn,i} k_i + A^{(0)}_{mn,i}, \quad i = x, y, z. \tag{S2-2}$$

To solve Eq. (7) numerically in real space using finite difference method (FDM), one should carefully cope with the uniformity of difference scheme. For the quantum well structure, we discuss the one-dimensional condition along z direction ([001]), the wave vector along the quantized direction is set to $k_z = -i\partial / \partial z$ as the differential operator to form like Eq. (6). Then recast the Hamiltonian into the form of k_z,

$$-\mathrm{H}(z)^{(2)} \frac{\partial^2 F(z)}{\partial z^2} - i\mathrm{H}(z)^{(1)} \frac{\partial F(z)}{\partial z} + \mathrm{H}(z)^{(0)} F(z) + U(z)F(z) = EF(z) \tag{S2-3}$$

In order to maintain the symmetry of Hamiltonian, the first-order difference operator is symmetrically processed into $\mathrm{H}(z)^{(1)} k_z = [\mathrm{H}(z)^{(1)} k_z + k_z \mathrm{H}(z)^{(1)}] / 2$. So we get the first-order difference form

$$\begin{aligned} & -\mathrm{H}(z)^{(2)} \frac{\partial^2 F(z)}{\partial z^2}\Big|_{z=z_i} \\ & \approx \frac{\mathrm{H}(z)^{(2)}{}_{i+1/2} F(z)_{i+1} - \left[\mathrm{H}(z)^{(2)}{}_{i+1/2} + \mathrm{H}(z)^{(2)}{}_{i-1/2}\right] F(z)_i + \mathrm{H}(z)^{(2)}{}_{i-1/2} F(z)_{i-1}}{-\Delta z^2}, \end{aligned} \tag{S2-4.1}$$

the second-order difference form

$$\begin{aligned} & -i\mathrm{H}(z)^{(1)} \frac{\partial F(z)}{\partial z}\Big|_{z=z_i} \\ & \approx -i \frac{\mathrm{H}(z)^{(1)}{}_{i+1/2} F(z)_{i+1} - \mathrm{H}(z)^{(1)}{}_{i-1/2} F(z)_{i-1}}{2\Delta z}, \end{aligned} \tag{S2-4.2}$$

and the zero-order term is

$$\left(\mathrm{H}(z)^{(0)}{}_i + U(z)_i\right)F(z) \tag{S2-4.3}$$

$\Delta z = z_{i+1/2} - z_{i-1/2}$ is the grid size, which represent the middle points of the current grid and the backward grid. The solution of the eigenfunction contains eight components

$$F(z)_i = \left[F(z)_{1,i}, F(z)_{2,i}, \mathrm{L}\ F(z)_{8,i}\right]^T \tag{S2-5}$$

Then the discretized Schrödinger equation is an 8N×8N matrix form of $\mathrm{F(z)}_i$, where $i = 1:\ N$. As a result, the discretized Schrödinger equation is arranged into a form of coefficient equation set concerning the adjacent points $(i-1, i, i+1)$.

$$\left(O_{i.i-1}O_{i,i}O_{i,i+1}\right)\begin{pmatrix} F(z)_{i-1} \\ F(z)_i \\ F(z)_{i+1} \end{pmatrix} = E\begin{pmatrix} F(z)_{i-1} \\ F(z)_i \\ F(z)_{i+1} \end{pmatrix} \tag{S2-6}$$

where

$$O_{i.i-1} = -\frac{1}{2\Delta z^2}\left(\mathrm{H}(z)^{(2)}{}_{i-1} + \mathrm{H}(z)^{(2)}{}_i\right) + \frac{1}{4\Delta z}\left(\mathrm{H}(z)^{(1)}{}_{i-1} + \mathrm{H}(z)^{(1)}{}_i\right)$$

$$O_{i.i} = \frac{1}{2\Delta z^2}\left(\mathrm{H}(z)^{(2)}{}_{i-1} - 2\mathrm{H}(z)^{(2)}{}_i + \mathrm{H}(z)^{(2)}{}_{i+1}\right) + \mathrm{H}(z)^{(0)}{}_i + U(z)_i \tag{S2-7}$$

$$O_{i.i+1} = -\frac{1}{2\Delta z^2}\left(\mathrm{H}(z)^{(2)}{}_{i+1} + \mathrm{H}(z)^{(2)}{}_i\right) - \frac{1}{4\Delta z}\left(\mathrm{H}(z)^{(1)}{}_{i+1} + \mathrm{H}(z)^{(1)}{}_i\right)$$

Apply Eq. (12) to the 8N×8N matrix, we can see

$$\begin{pmatrix} O_{1,1} & O_{1,2} & 0 & \mathrm{L} & 0 \\ O_{2,1} & O_{2,2} & O_{2,3} & & \mathrm{M} \\ 0 & O_{3,2} & \mathrm{O} & \mathrm{O} & \mathrm{M} \\ \mathrm{M} & & \mathrm{O} & \mathrm{O} & O_{N-1,N} \\ 0 & \mathrm{L} & 0 & O_{N,N-1} & O_{N,N} \end{pmatrix}\begin{pmatrix} F(z)_1 \\ F(z)_2 \\ \mathrm{M} \\ \mathrm{M} \\ F(z)_N \end{pmatrix} = E\begin{pmatrix} F(z)_1 \\ F(z)_2 \\ \mathrm{M} \\ \mathrm{M} \\ F(z)_N \end{pmatrix} \tag{S2-8}$$

Finally, the solution of the 8×8 Schrödinger equation of the specific quantum well can

be obtained by solving the above sparse large matrix.

S3. Analysis of the interaction between Au and semiconductor.

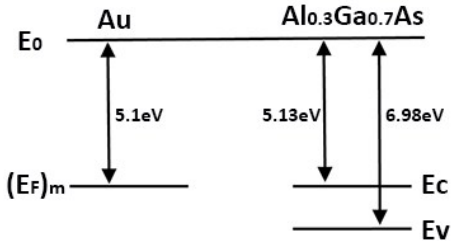

Figure S3-1. Band diagram before contact of Au and $Al_{0.3}Ga_{0.7}As$

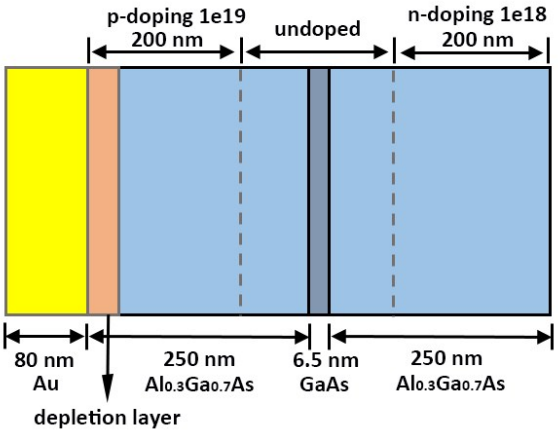

Figure S3-2. Schematic of the structure under equilibrium state

The Au layer is deposited on the QWNR to adjust the location of the neutral plane. We firstly consider the electron transfer caused by the difference of Fermi energy between Au and semiconductor, as shown in Figure S3-1. After contact, the electrons of Au flow to the $Al_{0.3}Ga_{0.7}As$, which form the built-in electric field at the interface. The maximum width of the depleted layer on the semiconductor side is 16.3 nm given by $W_{dep} = \sqrt{2\varepsilon_s \phi_{bi} / qN_a}$. The whole system quickly reached a thermal equilibrium

state after contact, as shown in Figure S3-2. The quantum well is in the neutral zone which is not affected.

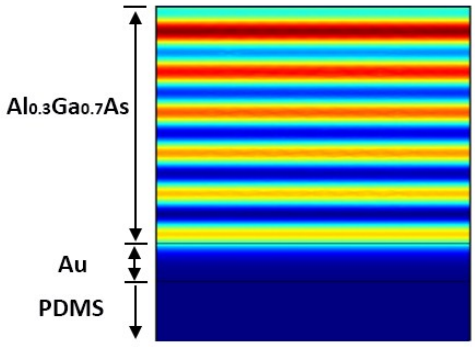

Figure S3-3. FEM analysis for the light absorption of QWNR

The light injection during the measurement caused non-equilibrium state of the system. We simulate the whole field of structure irradiated by the light source (λ = 633 nm) in the measurement by finite element method. Here, the GaAs layer is too thin to be neglected. Figure S3-3 shows the distribution of optical power loss. The result indicates that the light absorption is mainly concentrated in the $Al_{0.3}Ga_{0.7}As$ layer. The reflected light from the Au-$Al_{0.3}Ga_{0.7}As$ interface together with the incident light form the standing wave distribution. By integrating the absorption of each layer, we can get the light absorption of each layer of material. The reflectivity of the whole system is 48.7%, the absorptivity of the whole semiconductor layer is 49.4%, and the absorptivity of the gold layer is 1.6%. That is, the absorptivity of the semiconductor layer is approximately 30.8 times that of the gold layer. Supposing that all of the free electrons produced by the thermal excitation of gold was injected into the QW without recombination, the injection caused by gold is still far less than the injection caused by the semiconductor p-n junction. Therefore, the concentration of free electrons injected from gold into semiconductors is negligible for the optical

properties of QWNR.

S4. Analysis of radiative recombination process

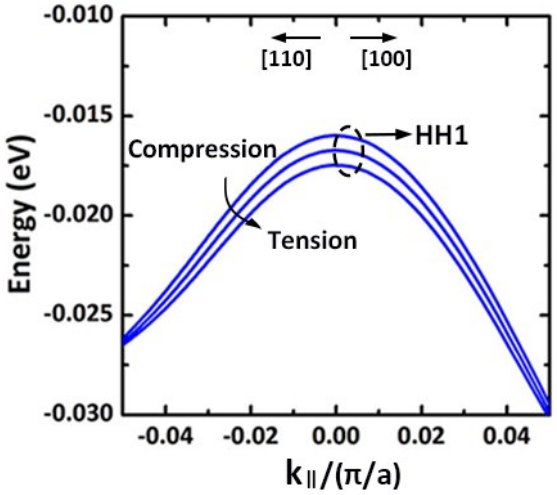

Figure S4-1. Dispersion curves of the highest valence band near the Γ point for different strain conditions, along [100] and [110] direction respectively.

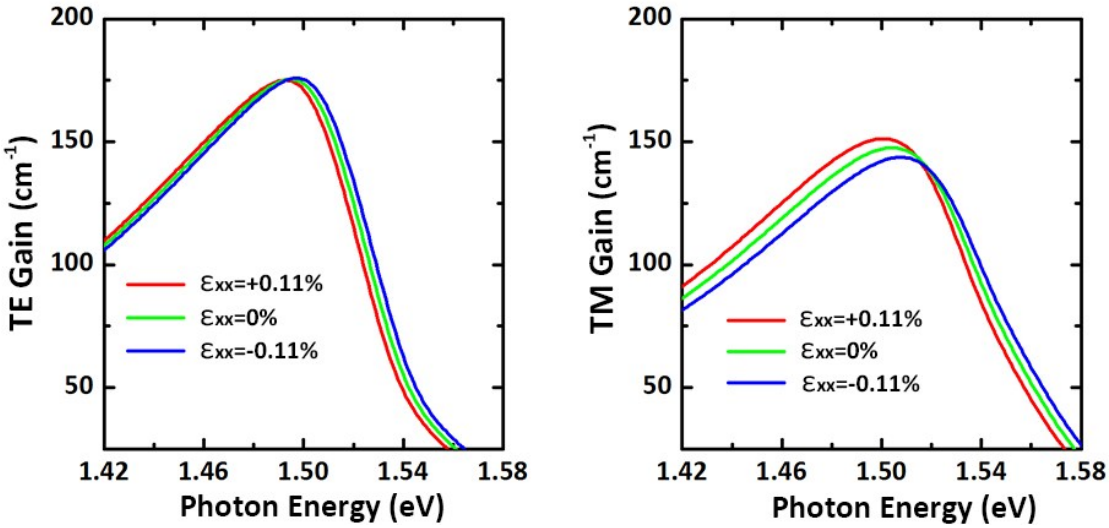

Figure S4-2. Material gain spectra of the GaAs/ $Al_{0.3}Ga_{0.7}As$/ GaAs QW for (a) TE and (b) TM under different strain conditions: $\varepsilon_{xx} = -0.11\%$, $\varepsilon_{xx} = 0\%$ and $\varepsilon_{xx} = 0.11\%$.

We can calculate TE and TM material gain spectra by the spontaneous emission

transformation method, taking into account the homogenous broadening by the Lorentzian function with a full-width-at-half-maximum (FWHM) linewidth γ.

$$g_{\mathrm{w}}^{\mathrm{TE}}(\mathsf{h}\omega) = C(\omega)\sum_{\sigma=\mathrm{U,L}}\sum_{\mathrm{n,m}}\int_0^{\infty}\frac{k_{\mathrm{t}}dk_{\mathrm{t}}}{2\pi}L(\mathsf{h}\omega)M_{\mathrm{nm}}^{\sigma,\mathrm{TE}}(k_{\mathrm{t}})\left[f_{\mathrm{n}}(k_{\mathrm{t}}) - f_{\mathrm{m}}^{\sigma}(k_{\mathrm{t}})\right] \tag{S4-1}$$

$$g_{\mathrm{w}}^{\mathrm{TM}}(\mathsf{h}\omega) = C(\omega)\sum_{\sigma=\mathrm{U,L}}\sum_{\mathrm{n,m}}\int_0^{\infty}\frac{k_{\mathrm{t}}dk_{\mathrm{t}}}{2\pi}L(\mathsf{h}\omega)M_{\mathrm{nm}}^{\sigma,\mathrm{TM}}(k_{\mathrm{t}})\left[f_{\mathrm{n}}(k_{\mathrm{t}}) - f_{\mathrm{m}}^{\sigma}(k_{\mathrm{t}})\right] \tag{S4-2}$$

where

$$L(\mathsf{h}\omega) = \frac{\gamma/\pi}{\left[E_{\mathrm{n}}(k_{\mathrm{t}}) - E_{\mathrm{m}}^{\sigma}(k_{\mathrm{t}}) - \mathsf{h}\omega\right]^2 + \gamma^2}, \tag{S4-3}$$

and

$$C(\omega) = \frac{\pi e^2}{\omega n_r c\varepsilon_0 m_0^2 L_{\mathrm{QW}}}. \tag{S4-4}$$

Here, n_r is the background refractive index, c is the speed of light in free space, ε_0 is the permittivity of free space, and $\mathsf{h}\omega$ is the photon energy. $f_{\mathrm{n}}(k_{\mathrm{t}})$ and $f_{\mathrm{m}}^{\sigma}(k_{\mathrm{t}})$ is the electron Fermi occupation number in the conduction and valence band. For quantum wells, the optical momentum matrix elements are polarization-dependent. By averaging the TE and TM momentum matrix elements in the plane of quantum wells, the average squared TE momentum matrix elements are given by,

$$M_{\mathrm{nm}}^{\mathrm{U,TE}}(k_{\mathrm{t}}) = \frac{3}{2}\left|\int_{-\infty}^{\infty}dz\phi_{\mathrm{n}}^{*}(z)M_{\mathrm{b}}g_{\mathrm{m}}^{(1)}(k_{\mathrm{t}},z)\right|^2 + \frac{1}{2}\left|\int_{-\infty}^{\infty}dz\phi_{\mathrm{n}}^{*}(z)M_{\mathrm{b}}g_{\mathrm{m}}^{(2)}(k_{\mathrm{t}},z)\right|^2 \tag{S4-5}$$

$$M_{\mathrm{nm}}^{\mathrm{L,TE}}(k_{\mathrm{t}}) = \frac{3}{2}\left|\int_{-\infty}^{\infty}dz\phi_{\mathrm{n}}^{*}(z)M_{\mathrm{b}}g_{\mathrm{m}}^{(4)}(k_{\mathrm{t}},z)\right|^2 + \frac{1}{2}\left|\int_{-\infty}^{\infty}dz\phi_{\mathrm{n}}^{*}(z)M_{\mathrm{b}}g_{\mathrm{m}}^{(3)}(k_{\mathrm{t}},z)\right|^2 \tag{S4-6}$$

$$M_{\mathrm{b}}^{2}=\frac{m_{0}}{6}E_{\mathrm{P}} \tag{S4-7}$$

Similarly, the average squared TM momentum matrix elements can be written as

$$M_{\mathrm{nm}}^{\mathrm{U,TM}}\left(k_{\mathrm{t}}\right)=2\left|\int_{-\infty}^{\infty}dz\phi_{\mathrm{n}}^{*}\left(z\right)M_{\mathrm{b}}g_{\mathrm{m}}^{(2)}\left(k_{\mathrm{t}},z\right)\right|^{2} \tag{S4-8}$$

$$M_{\mathrm{nm}}^{\mathrm{U,TM}}\left(k_{\mathrm{t}}\right)=2\left|\int_{-\infty}^{\infty}dz\phi_{\mathrm{n}}^{*}\left(z\right)M_{\mathrm{b}}g_{\mathrm{m}}^{(3)}\left(k_{\mathrm{t}},z\right)\right|^{2} \tag{S4-9}$$

where $\phi_{\mathrm{n}}\left(z\right)$ is the wavefunction of the *n*-th state in the Γ-conduction band; $g_{\mathrm{m}}^{(1)}$ and $g_{\mathrm{m}}^{(2)}$ ($g_{\mathrm{m}}^{(3)}$ and $g_{\mathrm{m}}^{(4)}$) are eigenfunctions of the upper (lower) block Hamiltonian of the HH1 and LH1 band; M_{b} is the bulk momentum matrix element.